JOURNAL OF SOLID STATE CHEMISTRY **127,** 359–362 (1996)
ARTICLE NO. 0395

LETTER TO THE EDITOR

Crystal Structure and Spin Gap State of CaV_2O_5

Masashige Onoda and Noriaki Nishiguchi

Institute of Physics, University of Tsukuba, Tennodai, Tsukuba 305, Japan

Communicated by J. W. Richardson November 12, 1996; accepted November 27, 1996

The crystal structure and electronic state of CaV_2O_5 have been explored through X-ray four-circle diffraction, magnetization, and ESR measurements. The crystal at 297 K is orthorhombic with space group *Pmmn* and the lattice constants are $a = 11.351$ (2) Å, $b = 3.604$ (1) Å, $c = 4.893$ (1) Å, and $Z = 2$. Full-matrix least-squares refinement gives the final values of $R = 0.044$ and $R_w = 0.034$ for 880 independent reflections with $R_{int} = 0.041$. The structure is described in terms of VO_5 pyramids which are joined by sharing edges and corners to form characteristic V zigzag chains along the *b*-axis. Along the *a*-axis, the zigzag chains are linked by sharing corners, leading to a quasi-two-dimensional layer. This compound has a spin-singlet ground state with a gap of 660 K and $g = 1.96$. © 1996 Academic Press

I. INTRODUCTION

Vanadium ternary oxides and bronzes with unfilled 3*d* orbitals often have phase transitions from paramagnetic to spin-singlet states. For example, a quasi-one-dimensional conductor bronze β-$Na_xV_2O_5$ with $x \simeq 1/3$ has a kind of charge-density-wave or the *bipolaronic state* associated with a V^{4+}–V^{4+} bonded pair (1). A triangular lattice conductor $LiVO_2$ has a V^{3+}–V^{3+} bonded cluster or the *trimerized state* (2). It is interesting to explore mechanisms for the electronic transports of these characteristic bound states, because in the study of high temperature superconductors, various magnetic anomalies are observed, which appear to be related by the existence of a spin gap. Spin gap for $S = 1/2$ antiferromagnetically coupled chains, such as those found in the ladder compound $(VO)_2P_2O_7$, has also been studied intensively (3).

Since the discovery of the characteristic spin-singlet state of CaV_4O_9 (4), electronic states of the CaV_nO_{2n+1} system with $n = 2$–4 (5–7) have been investigated (8–12). No detailed structure for $n = 2$ in this system has been determined. This work describes the detailed crystal structure determined by X-ray four-circle diffraction as well as the spin gap state of CaV_2O_5 revealed by magnetization and ESR measurements. The latter has preliminarily been reported elsewhere (11).

II. CRYSTAL STRUCTURE

Reddish-brown sintered specimens of CaV_2O_5 were prepared as follows: First, $CaVO_3$ was made according to the procedure described in Ref. (13) and V_2O_3 was reduced by heating V_2O_5 in a N_2/H_2 atmosphere at 973 K for 48 h, where $CaCO_3$ (99.99% purity) and V_2O_5 (99.99% purity) were used. Mixtures of $4CaVO_3$, V_2O_3, and V_2O_5 were ground and pressed into pellets and then sealed in quartz tubes which were heated at 1223 K for 24 h. This annealing was done twice with an intermediate grinding. Single crystals were obtained by annealing the sintered specimens at 1373 K for 30 days with several intermediate grindings under Ar atmosphere.

The single phase for the specimens was confirmed from X-ray powder diffraction patterns with CuKα radiation at 297 K using a Rigaku RAD-IIC diffractometer. Electrical resistivity for the sintered specimens at 294 K was 11 MΩcm. X-ray four-circle diffraction measurements were carried out at 297 K on a Rigaku AFC-7R diffractometer (custom-made) with graphite monochromated MoKα radiation. A crystal with dimensions $0.03 \times 0.03 \times 0.01$ mm was used. Intensity data for the structure analysis were collected using the ω-2θ scan technique. Based on the systematic absences of reflections for single crystal diffraction, a statistical analysis of intensity distribution, and the successful solution and refinement of the structure described later, the space groups and the lattice constants are determined as listed in Table 1. Various parameters for structure solutions and refinements are also summarized. Due to the small size of the crystal, no absorption correction has been applied. This was justified by azimuthal scans of several reflections.

The structure was solved by direct methods (14), expanded using Fourier techniques, and refined by the full-matrix least-squares calculations with anisotropic displacement parameters. Here, atomic scattering factors were

0022-4596/96 $18.00
Copyright © 1996 by Academic Press
All rights of reproduction in any form reserved.

TABLE 1
Crystal Data and Summary of Intensity Measurements, Structure Solutions, and Refinements of CaV_2O_5

Crystal system	Orthorhombic
Space group	*Pmmn* (No. 59)
Z value	2
a (Å)	11.351 (2)
b (Å)	3.604 (1)
c (Å)	4.893 (1)
V (Å^3)	200.2 (2)
$\mu_{MoK\alpha}$ (mm^{-1})	5.840
D_{cal} (Mg/m^3)	3.682
Radiation	Mo$K\alpha$
$2\theta_{max}$ (°)	120
No. unique reflections	1791
R_{int}	0.041
Correction	Lorentz polarization
Structure solution	Direct method (SAPI 90)
Refinement	Full-matrix least-squares
No. observations ($I > 3\sigma$)	880
No. variables	27
Reflection/parameter ratio	32.59
R^a	0.0435
$R_w{}^b$	0.0338

[a] $R = \Sigma \, ||F_o| - |F_c|| / \Sigma |F_o|$.
[b] $R_w = [\Sigma w(|F_o| - |F_c|)^2 / \Sigma \, wF_o{}^2]^{1/2}$.

taken from Cromer and Waber (15), and anomalous dispersion effects were included, for which the values were those of Creagh and McAuley (16). A table of observed and calculated structure factors has been deposited with the National Auxiliary Publications Service.[1] All calculations were performed using the teXsan crystallographic software package (17).

Atomic coordinates, equivalent isotropic thermal parameters, and anisotropic displacement parameters are listed in Table 2. Selected interatomic distances are listed in Table 3. As shown in Fig. 1, the structure is formed by a linkage of VO_5 pyramids having apex oxygens in the direction of the c-axis. Here, the displacement parameter of the V ion may be anisotropic due to the short distance of V–O1. Oxygen edge- and corner-shared zigzag V chains are formed along the b-axis, where the nearest neighbor distance is 3.03 Å. Along the a-axis, these chains are linked by sharing corners with the distance of 3.49 Å, and thus a quasi-two-dimensional layer exists in the ab-plane. Ca atoms are located between the layers and surrounded by eight O atoms. The present structure is found to be similar to that of α'-NaV_2O_5 with two kinds of VO_5 pyramids (18).

The V–V distances are too large for significant direct overlap of vanadium 3d wavefunctions. Thus, the electronic state of CaV_2O_5 should be discussed based on the critical overlap integral between the vanadium and oxygen atoms, namely the V–O bond lengths. Using the results of Table 3, the effective valence at the V site is estimated to be 4.0 in terms of the bond length versus bond strength relation (19). This value is consistent with V^{4+} ($3d^1$) expected from the chemical formula. Simple crystal field analysis with the Hartree–Fock function V^{4+} (20) for the VO_5 pyramid indicates that the ground state wavefunction of $3d^1$ electrons is composed of $0.864d_{xy} + 0.503d_{yz}$, where $x \| a$ and $y \| b$. An average of the Ca–O distance is 2.47 Å and the effective ionic radius of Ca is estimated to be 1.09 Å, a reasonable value for eight-coordinated Ca ions (21).

The alternative space group $P2_1mn$ with the same systematic absences should be tested. Full-matrix least-squares refinement based on this space group leads to the values of $R = 0.0415$ and $R_w = 0.0323$ with high correlation coefficients for the variables of V and O atoms, where the number of variables is 48. There exist two crystallographically independent VO_5 pyramids. In these pyramids, the bond lengths between V and the apex oxygen are signifi-

[1] A NAPS document number for the deposition of auxiliary material will be provided in a later issue.

TABLE 2
Atomic Coordinates,[a] Equivalent Isotropic Thermal Parameters B_{eq} (Å^2),[b] and Anisotropic Displacement Parameters $U_{ij}{}^c$ of CaV_2O_5

Atom	Site	x	z	B_{eq}	U_{11}	U_{22}	U_{33}	U_{13}
V	4f	0.40388(4)	0.3906(1)	0.462(5)	0.0038(1)	0.0054(1)	0.0084(1)	−0.0004(2)
Ca	2b	0.75	0.1559(2)	0.68 (1)	0.0084(3)	0.0074(3)	0.0101(3)	0
O1	4f	0.3772 (2)	0.0602(5)	0.97 (3)	0.0116(8)	0.0157(9)	0.0096(9)	−0.007(7)
O2	4f	0.5755 (2)	0.4656(5)	0.69 (3)	0.0047(6)	0.0068(7)	0.0148(9)	−0.0011(6)
O3	2a	0.25	0.5461(7)	0.61 (4)	0.0054(9)	0.009 (1)	0.009 (1)	0

[a] For all atoms, $y = 0.25$ and $U_{12} = U_{23} = 0$.
[b] $B_{eq} = \frac{8}{3}\pi^2[U_{11}(aa^*)^2 + U_{22}(bb^*)^2 + U_{33}(cc^*)^2 + 2U_{12}aa^*bb^*\cos\gamma + 2U_{13}aa^*cc^*\cos\beta + 2U_{23}bb^*cc^*\cos\alpha]$.
[c] $\exp[-2\pi^2(a^{*2}U_{11}h^2 + b^{*2}U_{22}k^2 + c^{*2}U_{33}l^2 + 2a^*b^*U_{12}hk + 2a^*c^*U_{13}hl + 2b^*c^*U_{23}kl)]$.

TABLE 3
Selected Interatomic Distances (Å) of CaV_2O_5

Metal ions		O1–O2	3.000 (3)
V–V	3.0257(8)	O1–O2′ (×2)	2.986 (3)
V–V′	3.493 (1)	O1–O3	2.781 (4)
V–Ca	3.3500(8)	O2–O2 (×2)	2.509 (3)
VO_5 pyramid		O2–O3 (×2)	2.679 (2)
V–O1	1.645 (2)	CaO_8 polyhedron	
V–O2	1.982 (2)	Ca–O1 (×4)	2.539 (2)
V–O2′ (×2)	1.949 (1)	Ca–O2 (×2)	2.494 (2)
V–O3	1.905 (1)	Ca–O3 (×2)	2.318 (2)

cantly different: 1.56 (1) Å and 1.73 (1) Å. The R_w factor ratio test (22) for a significance level of 0.005 indicates that this structure would be more reliable than that shown in Fig. 1. However, the standard deviations for atomic parameters are larger than those listed in Table 2. In addition, we obtain noninteger V valences of 4.5 and 3.7, which lead to the larger average valence than the expected value from the chemical formula. Therefore, the space group of *Pmmn* may be accepted.

III. MAGNETIC PROPERTIES

Magnetization measurement for the sintered specimens was done using a magnetic balance in the region between 4.2 and 1100 K with fields of up to 10 kG. The magnetization versus field (M–H) curve was linear above 50 K, while below this temperature it had a tendency to saturate gradually with increasing field. The temperature dependence of observed magnetic susceptibility χ between 50 and 1100 K is shown in the top of Fig. 2 by the cross. There is a round maximum at 400 K, while below 90 K, a Curie–Weiss-like tail χ_{CW} appears. This tail may come from the phase such as a lattice imperfection or a magnetic impurity that cannot be detected by standard X-ray powder diffraction, where Curie constant and Weiss temperature are estimated to be $5.9(2) \times 10^{-3}$ emu K/mol V and $-12(1)$ K, respectively. The saturation behavior of M–H curve below 50 K is found to be due to this phase whose spin concentration is about 2% for V^{4+}. Subtracting χ_{CW} and the constant paramagnetism ($\chi_0 = 2 \times 10^{-5}$ emu/molV) from the data, their contributions being shown by the dotted line in the top of Fig. 2, we obtain the intrinsic temperature-dependent behavior χ_d of CaV_2O_5 that is plotted in the top of Fig. 2 by the open circle. Thus, the ground state is found to be spin-singlet, which appears to be consistent with the NMR result published by another group (12).

X-band ESR was measured for the sintered specimens using a JEOL spectrometer in the region between 17 and 300 K. The line shape is a single Lorentzian with g =

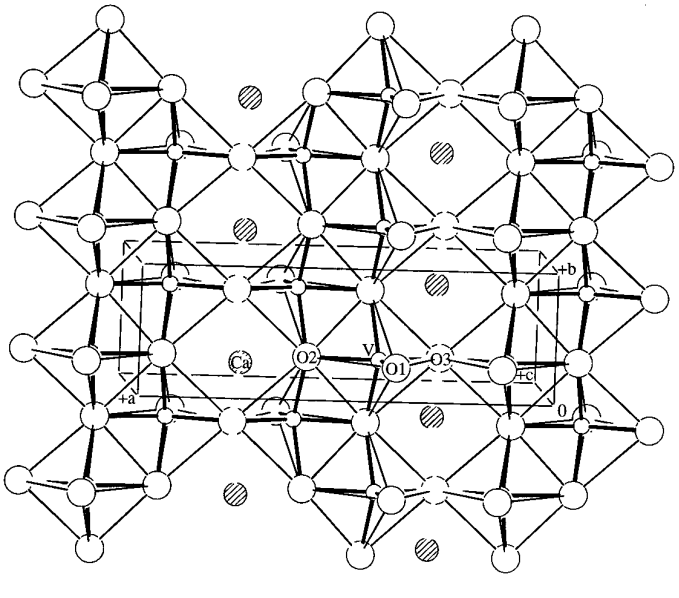

FIG. 1. Crystal structure of CaV_2O_5, where the unit cell box is displayed.

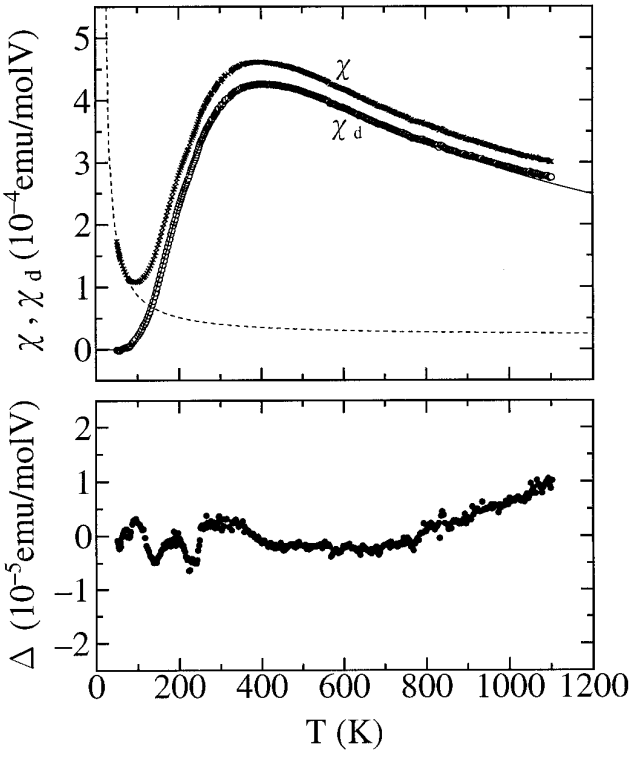

FIG. 2. Temperature dependence of the observed magnetic susceptibility χ (cross) and the intrinsic temperature-dependent one χ_d (open circle) of CaV_2O_5. The dotted line indicates the sum of the Curie–Weiss law χ_{CW} and the constant paramagnetism χ_0, and the solid line displays the dimer susceptibility χ_{dimer}. The difference Δ between χ_d and χ_{dimer} is plotted in the bottom.

1.957(1) and the extracted spin susceptibility nearly corresponds to the *intrinsic* behavior shown in the top of Fig. 2.

The dimer model, $\chi_{\text{dimer}} = Ng^2\mu_B^2/\{kT\,[\exp(E_g/T) + 3]\}$, where E_g is a singlet–triplet excitation gap, N is the number of V^{4+} ions, g is the g-factor, μ_B is the Bohr magneton, and k is Boltzmann constant, is found to be more appropriate than the model of quadratic energy dispersion with the finite gap (23) with regard to the temperature dependence of χ_d. The solid line in the top of Fig. 2 is for N = 0.98 mol, E_g = 664(1) K, and g = 1.957, that is, the ESR result. In the bottom of Fig. 2, the difference Δ between χ_d and χ_{dimer} is plotted. Above 700 K ($T > E_g$), Δ increases gradually with temperature. The present structural study at 297 K has revealed an absence of lattice distortion in the zigzag chain, indicating that the origin of the energy gap could be based upon the Heisenberg chain-like model with the next-nearest neighbor interaction that partially frustrates the nearest neighbor correlations (24).

IV. CONCLUSION

We have determined the crystal structure of CaV_2O_5 and measured the magnetic properties. This compound has a quasi-one-dimensional zigzag chain formed by the linkage of VO_5 pyramids along the b-axis. The corner linkage of the chains along the a-axis leads to a two-dimensional-like layer. The ground state of V^{4+} is an admixture of d_{xy} and d_{yz} orbitals. The electronic state is spin-singlet with a gap of 660 K and at the temperature region below this gap the temperature dependence of spin susceptibility corresponds well to that expected from the simple dimer model. The importance of the next-nearest neighbor interaction in the zigzag chain has been postulated.

In order to explore the anomalous magnetic properties of CaV_nO_{2n+1}, a high-temperature-series expansion study for the magnetic susceptibility is in progress.

ACKNOWLEDGMENTS

We thank Professor K. Kubo and Professor S. Takada for stimulating discussions and Mr. I. Miura and Mr. T. Miyata for their help in the early stage of experiments.

REFERENCES

1. M. Onoda and H. Nagasawa, *Phys. Status Solidi* B **141,** 507 (1987) and references therein.
2. M. Onoda and T. Inabe, *J. Phys. Soc. Jpn.* **62,** 2216 (1993) and references therein.
3. R. S. Eccleston, T. Barnes, J. Brody, and J. W. Johnson, *Phys. Rev. Lett.* **73,** 2626 (1994).
4. S. Taniguchi, T. Nishikawa, Y. Yasui, Y. Kobayashi, M. Sato, T. Nishioka, M. Kontani, and K. Sano, *J. Phys. Soc. Jpn.* **64,** 2758 (1995).
5. J-C. Bouloux and J. Galy, *Acta Crystallogr. B* **29,** 269 (1973).
6. J-C. Bouloux and J. Galy, *Acta Crystallogr. B* **29,** 1335 (1973).
7. J-C. Bouloux and J. Galy, *J. Solid State Chem.* **16,** 385 (1976).
8. N. Katoh and M. Imada, *J. Phys. Soc. Jpn.* **64,** 4105 (1995).
9. K. Ueda, H. Kontani, M. Sigrist, and P. A. Lee, *Phys. Rev. Lett.* **76,** 1932 (1996).
10. M. Troyer, H. Kontani, and K. Ueda, *Phys. Rev. Lett.* **76,** 3822 (1996).
11. T. Miyata, I. Miura, M. Onoda, and H. Nagasawa, "Abstracts of the Meeting of the Physical Society of Japan, 48th Annual Meeting," Part 3, p. 23. 1993. [In Japanese]
12. H. Iwase, M. Isobe, Y. Ueda, and H. Yasuoka, *J. Phys. Soc. Jpn.* **65,** 2397 (1996).
13. M. Onoda, H. Ohta, and H. Nagasawa, *Solid State Commun.* **79,** 281 (1991).
14. F. Hai-Fu, "SAPI 90: Structure Analysis Programs with Intelligent Control," Rigaku Corporation, Tokyo, 1990.
15. D. T. Cromer and J. T. Waber, *in* "International Tables for X-Ray Crystallography," (J. A. Ibers and W. C. Hamilton, Eds.), Vol. IV, Sec. 2, Kynoch Press, Birmingham, 1974.
16. D. C. Creagh and W. J. McAuley, *in* "International Tables for Crystallography" (A. J. C. Wilson, Ed.), Vol. C, Kluwer Academic, Boston, 1992.
17. "Crystal Structure Analysis Package," Molecular Structure Corporation, 1992.
18. A. Carpy and J. Galy, *Acta Crystallogr. B* **31,** 1481 (1975).
19. W. H. Zachariasen, *J. Less-Common Metals* **62,** 1 (1978).
20. A. J. Freeman and R. E. Watson, *in* "Magnetism" (G. T. Rado and H. Suhl, Eds.), Vol. II, Part A, Academic Press, New York, 1965.
21. R. D. Shannon, *Acta Crystallogr. A* **32,** 751 (1976).
22. W. C. Hamilton, *in* "International Tables for X-Ray Crystallography" (J. A. Ibers and W. C. Hamilton, Eds.), Vol. IV, Sec. 4, Kynoch Press, Birmingham, 1974.
23. M. Troyer, H. Tsunetsugu and D. Würtz, *Phys. Rev. B* **50,** 13515 (1994).
24. For example, A. Auerbach, "Interacting Electrons and Quantum Magnetism," Chap. 8. Springer-Verlag, New York, 1994.